Residual Harmonics in Voltage Unbalanced Power Systems

Lance G. Grainger, *Senior Member, IEEE,* and Roy C. Spencer, *Member, IEEE*

Abstract—**The analysis of residual harmonics requires combining linear and nonlinear analysis into a computer algorithm. The mathematical techniques are to apply state space methods to solve the nonlinear loads such as converters in a time domain format, analyze the resulting waveform with a Fourier analysis to convert the data to the frequency domain, and then solve the linear portion of the circuit with a linear algebra method, preferably utilizing sparsity techniques to speed the solution. The key model in a power system is that for the three-phase transformer. It is of consequence to note that the phase angle of any harmonic is a function both of the fundamental and of the particular harmonic.**

I. Introduction

When a power system with nonlinear loads operates under voltage unbalanced conditions, residual harmonics will appear in the system neutrals. These residual harmonics behave similarly to zero sequence currents and voltages in that they strongly affect communications and control circuits with noise. They also penetrate computerized control equipment through common mode noise mechanisms appearing on the ground planes. The term "residual harmonic" is not defined in general IEEE usage, but the term appears in Alberta utilities' harmonic regulations, which are among the most stringent in the world. Residual harmonics are defined as those harmonics which can be measured by placing a zero sequence style window current transformer around all three phases of a three-phase system. For harmonic loadings, these utilities will permit the magnitude of the telephone $I * T$ product resulting from residual harmonics to be approximately one-fifteenth of the allowable magnitude of the $I * T$ product arising from balanced harmonics. The regulations also require customers to comply with harmonic limits when preexisting voltage unbalance equals a 2% negative sequence voltage component.

To analyze residual harmonics is not a simple proposition. Systems must be modeled in great detail, and often the data gathering effort will make the cost of such analysis unattractive. Despite these difficulties, it is useful under certain circumstances to conduct such an analysis. While computer programs exist to analyze balanced harmonic conditions, there are few tools available to assist an engineer to calculate the residual harmonics. To meet the utility regulations requires creating a design tool which can model all three phases as well as the neutrals of power systems and their components. This paper will introduce an approach to computer modeling to solve residual harmonics.

The three-phase transformer has been described in detail by Gorman and Grainger [1], Arrillaga, Bradley, and Bodger [2], and Yacamini and de Oliveira [3]. It is the key model to be considered in any computer program, and it must accurately depict the phase shifts in sinusoidal waves used in the frequency domain when the transformation is of the delta-wye type.

It is useful to separate the power system into linear and nonlinear portions and analyze the two portions with different methods. A method of tearing networks as described by Brameller, John, and Scott [4] is readily applied by replacing the nonlinear (harmonic producing) loads with current sources, and performing analysis in the frequency domain for each harmonic frequency of interest. The nonlinear portions of the network can be solved in the time domain with state space methods as described by Xia and Heydt in their appendix to [5], and the waveforms converted to the frequency domain by means of Fourier analysis. An interactive algorithm similar to that suggested by Kitchin [6] is required to provide an iterative convergence in voltage and current at the boundary points between the linear and nonlinear portions of the circuit.

As this method requires a tremendous amount of computer work, the solution method selected must be fast and efficient. One approach described by Brameller, Allan, and Haman [7] is to apply sparsity directed programming to the Zollenkopf bifactorization method of inverting a matrix.

These various ideas are synthesized in this paper to create a solution algorithm.

II. Applying Zollenkopf's Bifactorization Method

When a power system has its components interconnected, the busses are directly joined together by relatively few branches. This results in a matrix of the admittances containing a large number of zeros. Computer

Paper PID 94-17, approved by the Petroleum and Chemical Industry Committee of the IEEE Industry Applications Society for presentation at the 1993 Petroleum and Chemical Industry Committee Technical Conference, St. Louis, Missouri, Sept. 13, 1993. Manuscript released for publication May 4, 1994.

L. G. Grainger is President of Grainger Electrical Research Ltd., 8603-16th Avenue, Edmonton, Alberta, Canada T6K 2A4.

R. C. Spencer is at Interprovincial Pipe Line Inc., 10201 Jasper Avenue, P.O. Box 398, Edmonton, Alberta, Canada T5J 2J9.

IEEE Log Number 9404049.

programmers have utilized this fact for decades to reduce the storage requirements for data. Mathematicians like Zollenkopf have devised sparsity directed methods of matrix manipulation which avoid generation and storage of matrices containing a large number of elements. Thus the zero elements (which essentially contain no data but are of topological interest) have incurred a fair amount of thought and interest as to how to best use them. In solving power problems, it is useful to invert admittance matrices to obtain impedance matrices:

$$Z_{\mathrm{BUS}} = [Y_{\mathrm{BUS}}]^{-1}. \tag{1}$$

This has been done by several methods, one of the more popular being the LDH (Lower-Diagonal-Higher) triangulariation and another the Zollenkopf bifactorization. When one combines the triangularization factors, one forms the original Y_{BUS}, whereas combining the bifactorization factors results in obtaining the inverse. The computational and storage requirements for either method are similar, if a full Z_{BUS} is required, but the bifactorization method can be modified to obtain one column of the inverse at a time and advantage can be taken of the order in which the factorization matrices are created to require storage of results for only those busses supplying nonlinear loads. In a typical power system, this achieves a considerable saving in computational effort.

Showing the factorization steps by means of superscripts, the Zollenkopf method uses the fact that any matrix can be reduced one row and one column at a time by factoring out row and column factorization matrices:

$$C^{(1)}Y_{\mathrm{BUS}}R^{(1)} = Y^{(1)}, \tag{2}$$

$$C^{(2)}Y^{(1)}R^{(2)} = Y^{(2)}, \tag{3}$$

$$\vdots$$

until at step N (corresponding to the number of columns in the matrix), we obtain the unity matrix:

$$Y^{(N)} = U. \tag{4}$$

But

$$Y^{(N)} = C^{(N)} \cdots C^{(K)} \cdots C^{(1)}Y_{\mathrm{BUS}}R^{(1)} \cdots R^{(K)} \cdots R^{(N)} = U, \tag{5}$$

and premultiplying by the inverses of the column factors, then postmultiplying by the column factors in reverse order, gives

$$Y_{\mathrm{BUS}}R^{(1)} \cdots R^{(K)} \cdots R^{(N)}C^{(N)} \cdots C^{(K)} \cdots C^{(1)} = U; \tag{6}$$

then premultiplying both sides by Y_{BUS}^{-1} obtains the inverse matrix

$$R^{(1)} \cdots R^{(K)} \cdots R^{(N)}C^{(N)} \cdots C^{(K)} \cdots C^{(1)} = Y_{\mathrm{BUS}}^{-1}, \tag{7}$$

where the factorization matrices for step "K" are

$$C^{[K]} = \begin{bmatrix} 1 & \cdot & \cdot & C_{1K} & \cdot & \cdot \\ \cdot & 1 & \cdot & C_{JK} & \cdot & \cdot \\ \cdot & \cdot & 1 & \vdots & \cdot & \cdot \\ \cdot & \cdot & \cdot & C_{KK} & \cdot & \cdot \\ \cdot & \cdot & \cdot & \vdots & 1 & \cdot \\ \cdot & \cdot & \cdot & C_{NK} & \cdot & 1 \end{bmatrix},$$

$$R^{[K]} = \begin{bmatrix} 1 & \cdot & \cdot & \cdot & \cdot & \cdot \\ \cdot & 1 & \cdot & \cdot & \cdot & \cdot \\ \cdot & \cdot & 1 & \cdot & \cdot & \cdot \\ R_{K1} & \cdots & R_{KJ} & 1 & \cdots & R_{KN} \\ \cdot & \cdot & \cdot & \cdot & 1 & \cdot \\ \cdot & \cdot & \cdot & \cdot & \cdot & 1 \end{bmatrix}, \tag{8}$$

the column factor elements are

$$C_{JK}^{[K]} = \frac{-Y_{JK}^{[K-1]}}{Y_{KK}^{[K-1]}}, \qquad C_{KK}^{[K]} = \frac{1}{Y_{KK}^{[K-1]}}, \tag{9a}$$

the row factor elements for a symmetrical matrix are

$$R_{KJ}^{[K]} = C_{JK}^{[K]}, \qquad K \neq J, \quad R_{KK} = 1, \tag{9b}$$

and the reduced matrix elements are

$$Y_{IJ}^{[K]} = Y_{IJ}^{[K-1]} - \frac{Y_{IK}^{[K-1]}Y_{KJ}^{[K-1]}}{Y_{KK}^{[K-1]}}. \tag{10}$$

Zollenkopf stops at this point, and were we to do the same we would have achieved a fast method of computing the inverse, but we also would be faced with storing a very large Z_{BUS} matrix. An examination of an industrial power system will often reveal that there are very few busses supplying harmonic loads, hence there are few points at which harmonic current is injected into the system. One obvious point is the connection to the utility. Other points are the large rectifier loads and variable frequency drives. For example, in a power system with the incoming bus (1) and three other busses (L), (J), and (K) supplying harmonic loads, we need only concern ourselves with finding four columns of the Z_{BUS} matrix, namely column 1, column L, column J, and column K, and further require only the injected currents I_1, I_L, I_J, and I_K to solve all the bus voltages.

Z_{BUS} can be found one column at a time by multiplying the factors of the inverse (7) times the appropriate column of the unity matrix U. To find, for example, the Kth column:

$$\begin{bmatrix} Z_{1K} \\ \vdots \\ Z_{KK} \\ \vdots \\ Z_{NK} \end{bmatrix} = R^{(1)} \cdots R^{(k)} \cdots R^{(n)} C^{(n)} \cdots C^{(k)} \cdots C^{(1)} \begin{bmatrix} 0 \\ \vdots \\ 0 \\ 1 \\ 0 \\ \vdots \\ 0 \end{bmatrix}. \tag{11}$$

In implementing the above, a dynamic ordering technique is employed in which, at each step of factorization, the reduced matrix is searched for the unfactorized column containing the fewest elements, and this column is then factorized next. This method keeps the reduced matrix sparse. Modifying this procedure to factorize the harmonic load busses last eliminates all the column factors in (11) except those for the harmonic busses. For the example, only column factors for the harmonic load busses 1, J, K, and L need be considered, provided these busses are factorized as steps $N-3$, $N-2$, $N-1$, and N. This is made possible because multiplying a column factorization matrix of the "J" column by the "K" column of U results in the "K" column of U. The row factors have a different topology and all of them must be included:

$$\begin{bmatrix} Z_{1K} \\ \vdots \\ Z_{KK} \\ \vdots \\ Z_{NK} \end{bmatrix} = R^{(1)} \cdots R^{(K)} \cdots R^{(N)} C^{(N)} C^{(N-1)} \cdot C^{(N-2)} C^{(N-3)} \begin{bmatrix} 0 \\ \vdots \\ 0 \\ 1 \\ 0 \\ \vdots \\ 0 \end{bmatrix}. \tag{12}$$

Finally, to solve the particular example with current injected at the four busses 1, J, K, and L:

$$\begin{bmatrix} V_1 \\ V_2 \\ \vdots \\ \vdots \\ V_N \end{bmatrix} = \begin{bmatrix} Z_{11} \\ Z_{21} \\ \vdots \\ \vdots \\ Z_{N1} \end{bmatrix} \cdot I_1 + \begin{bmatrix} Z_{1J} \\ Z_{2J} \\ \vdots \\ \vdots \\ Z_{NJ} \end{bmatrix} \cdot I_J + \begin{bmatrix} Z_{1K} \\ Z_{2K} \\ \vdots \\ \vdots \\ Z_{NK} \end{bmatrix} \cdot I_K + \begin{bmatrix} Z_{1L} \\ Z_{2L} \\ \vdots \\ \vdots \\ Z_{NL} \end{bmatrix} \cdot I_L. \tag{13}$$

This process has to be repeated for each harmonic of interest, hence preserving sparsity is important. In an industrial plant, the first 80 harmonics must be solved to comply with the utility regulations in Alberta, so this requires storing the contents of 80 voltage vectors. It is the use of sparsity methods that makes the calculation possible on microcomputers.

III. Four-Port Transformer Model

To establish a matrix topology that will correctly handle the phase shifts for a delta-wye transformer requires the development of a transformer model with four nodes for each HV/LV winding pair associated with a particular core (see Fig. 1). Two of the nodes are across the primary winding and two of the nodes are across the secondary winding. It is not necessary to include the magnetizing branches in the model, as these can be added later as injected harmonic current sources. The simplest place to start is to consider only the transformer leakage admittance y, which is the inverse of the transformer nameplate impedance. This is referred to by some authors as the "primitive" admittance, and it can be described in matrix form by

$$Y_{\text{PRIM}} = \begin{bmatrix} y & -y \\ -y & y \end{bmatrix}. \tag{14}$$

It is necessary to modify this primitive matrix to accommodate the fact that the primary per-unit voltage α and the secondary per-unit voltage β may differ from line to neutral voltage:

$$Y_{\text{PRIM}} = \begin{bmatrix} \frac{1}{\alpha} & 0 \\ 0 & \frac{1}{\beta} \end{bmatrix} \begin{bmatrix} y & -y \\ -y & y \end{bmatrix} \begin{bmatrix} \frac{1}{\alpha} & 0 \\ 0 & \frac{1}{\beta} \end{bmatrix} = \begin{bmatrix} \frac{y}{\alpha^2} & -\frac{y}{\alpha\beta} \\ -\frac{y}{\alpha\beta} & \frac{y}{\beta^2} \end{bmatrix}. \tag{15}$$

This primitive matrix may be thought of as representing the two "hot" terminals of a winding, one on the primary and one on the secondary, with the voltages being between the terminals and reference. These voltages are similar to the branch voltages across the winding of a two-winding transformer. To develop a connection matrix showing the relationship between the branch and nodal voltages, consider the model in Fig. 1.

By inspection, the voltage across the branch can be related to the voltage at the nodes:

$$\begin{aligned} V_\alpha &= V_A - V_C, \\ V_\beta &= V_X - V_N, \end{aligned} \tag{16}$$

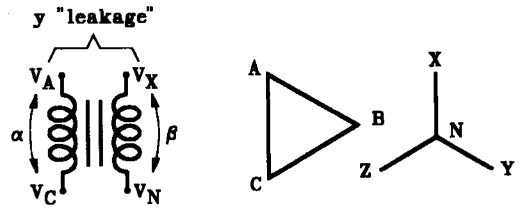

Fig. 1. Two-winding transformer showing node and branch voltages on one core.

or in matrix form,

$$\begin{bmatrix} V_\alpha \\ V_\beta \end{bmatrix} = \begin{bmatrix} 1 & -1 & 0 & 0 \\ 0 & 0 & 1 & -1 \end{bmatrix} \begin{bmatrix} V_A \\ V_C \\ V_X \\ V_N \end{bmatrix}, \tag{17}$$

thus creating the connection matrix,

$$C = \begin{bmatrix} 1 & -1 & 0 & 0 \\ 0 & 0 & 1 & -1 \end{bmatrix}. \tag{18}$$

By applying topological considerations,

$$Y_{\text{NODE}} = C^T Y_{\text{PRIM}} C, \tag{19}$$

which can be solved as

$$Y_{\text{NODE}} = \begin{bmatrix} \frac{y}{\alpha^2} & -\frac{y}{\alpha^2} & -\frac{y}{\alpha\beta} & \frac{y}{\alpha\beta} \\ -\frac{y}{\alpha^2} & \frac{y}{\alpha^2} & \frac{y}{\alpha\beta} & -\frac{y}{\alpha\beta} \\ -\frac{y}{\alpha\beta} & \frac{y}{\alpha\beta} & \frac{y}{\beta^2} & -\frac{y}{\beta^2} \\ \frac{y}{\alpha\beta} & -\frac{y}{\alpha\beta} & -\frac{y}{\beta^2} & \frac{y}{\beta^2} \end{bmatrix}. \tag{20}$$

By recalling that off-diagonal elements of an admittance matrix are the negative values of the transfer admittances, a network circuit can be "reverse engineered" by inspection of the above matrix to arrive at the circuit in Figure 2.

This model contains negative circuit elements with no real world parallel, but it has the virtue that it can be connected in the same manner as any pair of real world transformer windings to obtain wye-wye, delta-wye, or delta-delta configurations. While mutual coupling between transformer cores is neglected by this model, laboratory measurement has shown the admittance of such mutuals to be of the order of 3% of the leakage admittance, hence you can neglect them and still obtain valid results.

IV. Transformer Magnetizing Branch Model

The magnetizing branch of the transformer is nonlinear and can be modeled by injected current harmonics. This model is needed for those transformers supplying loads with a dc component. For other transformers it can be neglected. The data required for the model are obtained

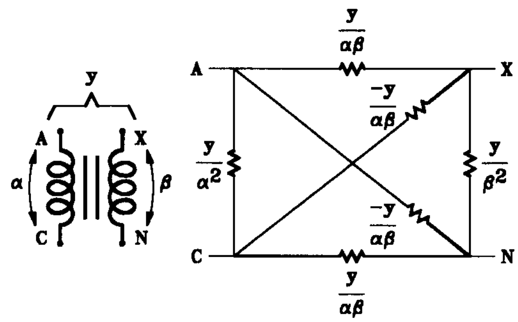

Fig. 2. Four-port admittance model of transformer.

from the transformer open circuit test by recording the instantaneous magnetizing current and excitation voltage across one cycle. The voltage is integrated to obtain excitation flux linkage, which is then plotted against the current to obtain the transformer magnetization curve. See Fig. 3.

This curve is then given a dc bias based upon the dc load current, the transformer turns ratio, and the slope of the magnetization curve at its extremities. Subsequent projection of the integrated ac voltage against the biased curve will result in a plot of the magnetization current present when a transformer feeds a dc load. This work is simplified if one uses a portable digital scope which has the capability to download real time data to a computer.

Magnetizing flux therefore has two forcing functions, the ac voltage and the dc load current:

$$\lambda = \int v \, dt + \lambda_{\text{DC}}. \tag{21}$$

The nonlinear components of a power system can be solved by a state variable method. In its essence the method depends upon being able to select appropriate "state variables" which are continuous functions (i.e., not subject to sudden step changes). Obvious candidates are voltages across capacitors and current through inductors. The method uses small time steps to obtain the approximation:

$$\frac{dx}{dt} \cdot \Delta t \approx \Delta x. \tag{22}$$

Better methods, such as the modified Euler or the fourth-order Runga–Kutta would be employed in the programming; the Euler method is shown here for brevity. Changes in the variable x can then be computed iteratively with the recursive form

$$x_{(k+1)} = x_{(k)} + \Delta x_{(k)}. \tag{23}$$

The method can predict the magnetizing current in a transformer from system voltage and a parabolic model of the saturation curve. Froelich's equation for flux linkage and magnetizing current i_M, where k_1, k_2 are derived constants, can be created by selecting two points on the

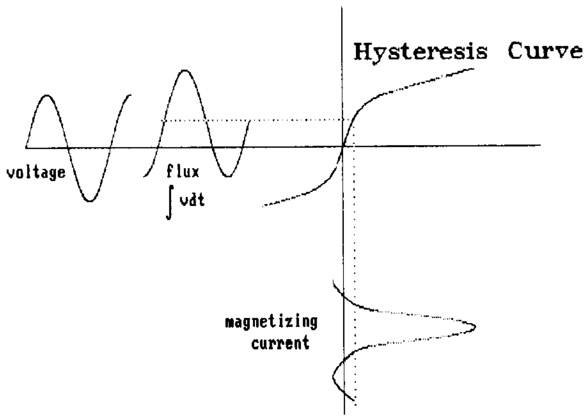

Fig. 3. Transformer flux offset due to dc load current.

curve, one near the knee and one where the flux linkage peaks:

$$\lambda = \frac{k_1 i_M}{k_2 + i_M}, \quad (24)$$

$$\frac{d\lambda}{di_M} = \frac{k_1 k_2}{(k_2 + i_M)^2}, \quad (25)$$

$$v = \frac{d\lambda}{dt} = \frac{d\lambda}{di_M} \cdot \frac{di_M}{dt}. \quad (26)$$

Rearrange (26):

$$\frac{di_M}{dt} = \frac{v}{\left(\frac{d\lambda}{di_M}\right)} \quad (27)$$

for small time increments

$$\Delta i_M = \frac{di_M}{dt} \cdot \Delta t; \quad (28)$$

rearrange (28):

$$\Delta\lambda = \frac{d\lambda}{dt} \cdot \Delta t = v \cdot \Delta t; \quad (29)$$

solve recursively:

$$i_{M(k+1)} = i_{M(k)} + \Delta i_{M(k)}, \quad (30)$$

$$\lambda_{(k+1)} = \lambda_{(k)} + \Delta\lambda_{(k)}. \quad (31)$$

The resulting curves are in the time domain and must be converted to the frequency domain by a Fourier method to obtain the current harmonics to be injected into the Y_{BUS} admittance matrix.

When considering the dc component of the load, it is necessary to consider the intercore dc coupling. Whereas the ac intercore coupling was considered negligible, the dc intercore coupling is quite strong. This is because dc flux in one core will complete a magnetic loop in the iron core of the transformer. Should a dc load be connected between any two secondary lines, the dc flux will circulate in the two affected cores, being positive in sign in one core and negative in sign in the other core. However, should the dc load be connected between one line and neutral, the dc flux created in that core will approximately divide between the other two cores. Thus a single-phase dc load will create harmonics in the primary currents of all three phases of a three-phase transformer.

Measurements taken on a three-phase core-type transformer give the wave forms shown in Fig. 4. With no load, the excitation current is approximately symmetrical in its positive and negative lobes. However, when a half wave rectifier is applied, the dc flux drives the transformer into saturation during one half of the cycle, while tending to let it operate in a more linear region during the opposite half cycle. This is shown in Fig. 5. It is also worth noting that a positive dc current results in a negative dc flux.

This behavior is incorporated into the model by reflecting the dc current through the magnetization curve to obtain dc flux. It is, however, important to reflect it through the slope that exists where the ac excitation current would have peaked had no direct current been present. In other words, the more the ac voltage drives the peaks of the excitation flux into saturation, the less is the offset afforded by the dc flux component.

Since the dc load cannot be "transformed," its net effect is to appear as even harmonics in the transformer primary excitation current. This will show up for single-phase loads such as the switch mode power supplies on computers, printers, photocopiers, televisions, and fax machines, and it will also appear on controlled rectifiers where the firing angle controller is permitting the positive lobe duration of current to be of a different duration than the negative lobe duration. This latter phenomenon will usually affect two input line currents to the rectifier, creating a positive dc current component in one and a negative dc component in the other. A comparison can be made between Fig. 6, which shows normal excitation current, and Fig. 7, which shows the change in the primary excitation of phases B and C when only the A phase secondary is loaded with a half wave rectifier. These dc components create dc flux in the rectifier transformers' secondaries, which creates even harmonics on the primary side. To reduce the amount of computational effort, only transformers supplying these loads should have the magnetizing branches modeled as harmonic current sources. For other transformers the magnetizing branches should be ignored.

V. Fundamental Voltages and Currents

To provide a reference phase angle for the injected harmonics, it is necessary to establish the phase angles of the fundamental currents. In the frequency domain, the angles of the harmonic components depend upon two things. The first is the relative phase angle of the fundamental with respect to some arbitrary system reference and the second is its own angular displacement at the harmonic frequency. This is better understood by examin-

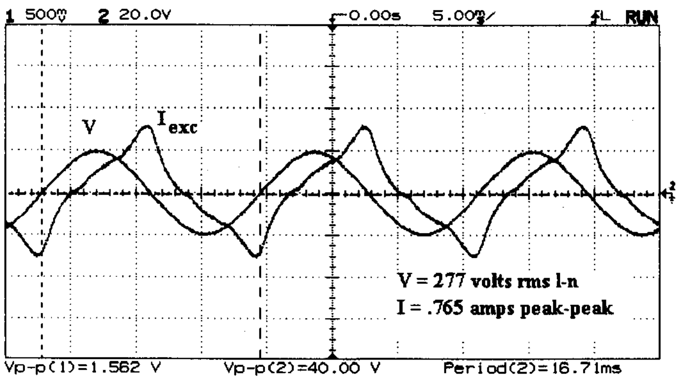

Fig. 4. Primary sinusoidal voltage and normal excitation current.

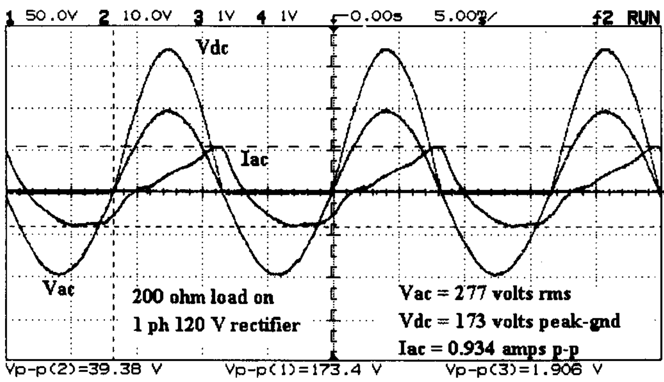

Fig. 5. Primary voltage and current and secondary diode voltage with half wave rectifier load on secondary.

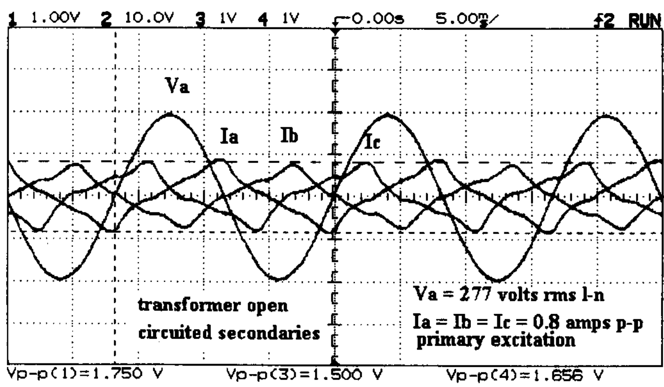

Fig. 6. Primary excitation currents and a phase voltage with all secondaries open circuited.

ing a typical formula for a harmonic series:

$$f(\omega t) = Q_{\mathrm{dc}} + \sum_{h=0}^{n} \left[Q_h \cos h(\omega t - \phi_1) + \phi_h \right], \quad (32)$$

where

- Q = magnitude of the harmonic term,
- h = harmonic order,
- ωt = fundamental frequency · time product,
- ϕ_1 = fundamental phase shift with respect to reference angle,
- ϕ_h = harmonic phase shift.

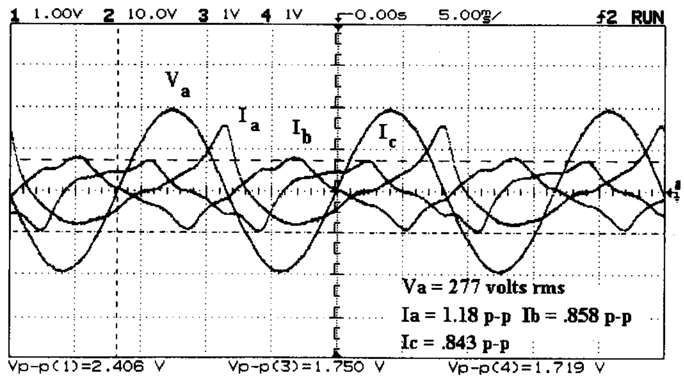

Fig. 7. Single-phase half wave rectifier on phase A causes distortion in primary current of all phases.

It is necessary to run a three-phase load flow at the fundamental frequency to establish the fundamental phase shift of voltage and current on each bus. Linear loads may be modeled in the traditional fashion of specifying the watts and vars at each bus. The nonlinear loads have to be subjected to a preliminary state space analysis to estimate the current and voltage at the fundamental frequency, hence the resulting watts and vars at the fundamental frequency can be estimated. To obtain a starting value for the study, losses can be neglected in nonlinear loads.

Having thus established the relative angles of current and voltage at each bus, subsequent harmonic calculations may proceed.

VI. Applying Diakoptic Methods

From a computational perspective, using time domain state space methods is slower than using frequency domain matrix inversion techniques. It is advantageous to divide the network into linear and nonlinear portions so that each portion may be solved by the most applicable method. This division may be accomplished by tearing the network at the busses supplying nonlinear loads, and by replacing the nonlinear loads with harmonic current sources. Similarly, those transformers associated with loads having a dc component of load current may have the magnetizing branches added by modeling them with harmonic current sources. See Fig. 8.

Because the fundamental watts and vars of the nonlinear loads will change depending on the voltage of the busses supplying them, and likewise the voltage at the busses depends upon the magnitudes of the harmonics flowing through and creating distorted voltage drops in the upstream impedances, an iterative solution is called for. The flowchart for a computer algorithm to accomplish this is given in Appendix B.

As the admittance matrix is formulated for each harmonic, the appropriate adjustments must be made in the admittance values to compensate for skin effect and the change in frequency. Skin effect will not only increase component resistance, but will also decrease the conductor internal flux linkages, hence reduce the total conductor inductance. As reactance becomes dominant in cir-

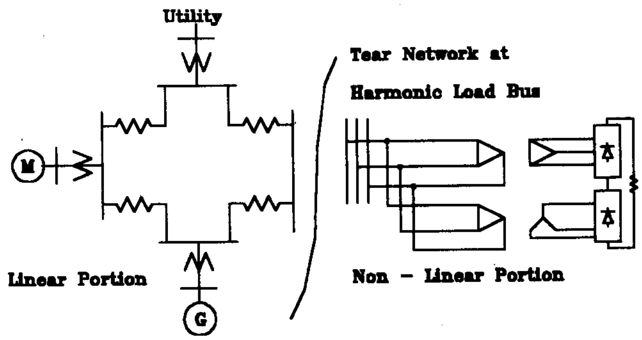

Fig. 8. Network torn into linear and nonlinear portions.

cuits at the higher frequencies, ignoring skin effect could lead to large errors in calculating system impedances. The skin effect of a 5-kV, three-conductor, 500-kcmil cable is shown in Appendix A.

VII. Conclusion

To model and analyze residual harmonics in unbalanced systems requires the synthesis of several techniques. A method has been described that uses easily obtained data for most of the models. The exception to this is the transformer magnetizing curve, which must be measured from an open circuit test. With the assistance of this computer tool, it becomes possible to assess probable causes for residual harmonics, and to test possible solutions to mitigating them.

It is worth noting that what requires an intense theoretical effort on the computer can be achieved simply in the field by measuring residual harmonics with a zero sequence style current transformer which surrounds either the three phases or alternatively the neutral conductor. Our work has shown that caution is advisable when measuring transformer primary currents, as improper application of Fourier transform techniques in various instruments can result in false readings of even harmonics. Observed low levels of even harmonics may in fact just be instrument artifacts. If, however, the even harmonics do exist, it is indicative of a dc load component on the transformer secondary.

Unbalanced systems are particularly susceptible to residual harmonics, as they tend to cause firing unbalance in what would otherwise be balanced three-phase loads. In turn, residual harmonics cause greater coupling with communications circuits than do balanced harmonics because they behave very similarly to zero sequence currents in power systems. Coupling interference due to a residual harmonic is 10 to 20 times as strong as it is for a balanced harmonic of similar magnitude. For these reasons Wye-type power distribution systems propagate residual harmonic related interferences.

The rationale for using the computer is in developing solutions to system problems. It is far cheaper to model residual harmonics for the purpose of predicting system behavior in conjunction with alternative solutions than to attempt to apply hardware on a trial and error basis. Measurement of residual harmonics and various solutions to mitigate them will be the subjects of future papers.

Appendix A

Skin Effect Ratios—5-kV-3^C 500-kcmil Cable

Harmonic Order	Resistance Ratio (DC=1)	Inductance Ratio (DC=1)
1	1.018	.998
5	1.344	.964
7	1.545	.944
11	1.887	.915
13	2.030	.905
17	2.281	.890
19	2.394	.884
23	2.604	.875
25	2.703	.872

Appendix B

Computer Program Flow Chart References

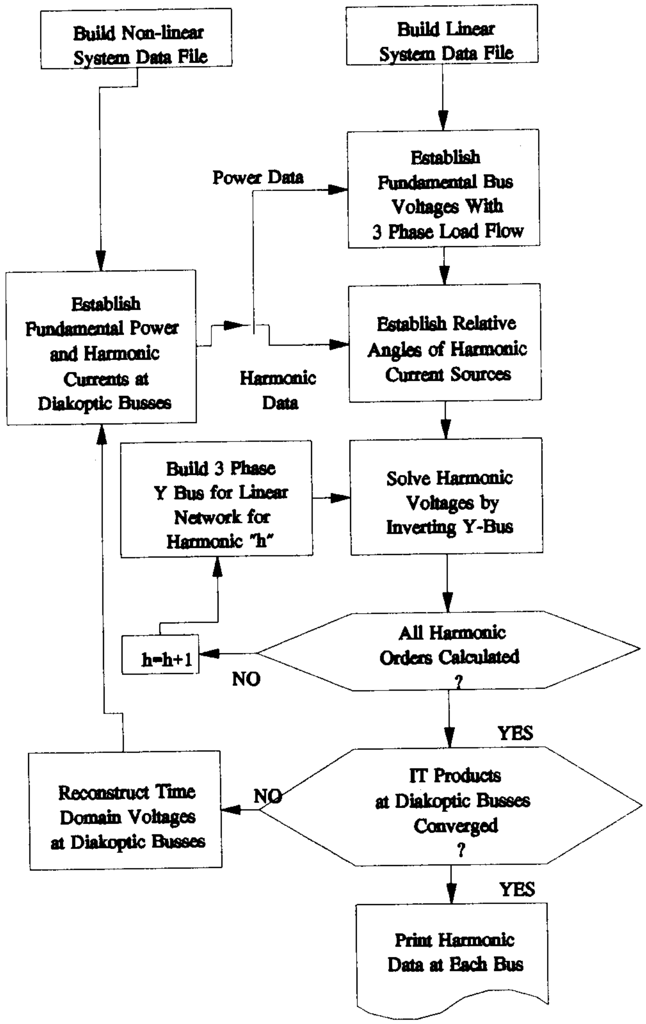

REFERENCES

[1] M. Gorman and J. J. Grainger, "Transformer modelling for distribution system studies—Part I—Linear modelling basics; Part II—Addition of models to Ybus and Zbus," *IEEE Power Eng. Soc. Transmission Distribution Conf. Rec.*, Sept. 1991, pp. 539–552.

[2] J. Arrillaga, D. A. Bradley, and P. S. Bodger, *Power System Harmonics*. Toronto: Wiley, 1985.

[3] R. Yacamini and J. C. de Oliveira, "Harmonics produced by direct current in converter transformers," *Proced. IEE (U.K.)*, vol. 125, no. 9, pp. 873–878, Sept. 1978.

[4] A. Brameller, M. N. John, and M. R. Scott, *Practical Dialoptics For Electrical Networks*. London: Chapman & Hall Ltd., 1969.

[5] D. Xia and G. T. Heydt, "Harmonic power flow studies Part I—Formulation and solution," *IEEE Trans. Power Applicat. Syst.*, vol. PAS-101, no. 6, pp. 1257–1266, June 1982.

[6] R. H. Kitchin, "New method for digital-computer evaluation of converter harmonics in power systems using state variable analysis," *Proced. IEE (U.K.)*, vol. 128, pt. C, no. 4, pp. 196–207, July 1981.

[7] A. Brameller, R. N. Allan, Y. M. Haman, *Sparsity—Its Practical Application to System Analysis* Toronto, Pitman Publishing, 1976.

Lance G. Grainger (SM'91) received the B.Sc. degree in electrical engineering from the University of Saskatchew in 1968, and the M.Eng. degree in electrical engineering from the University of Alberta in 1990.

He has worked in the utility, pulp and paper, petrochemical, mining, cement, pipeline, and consulting industries, and is president of Grainger Electrical Research Ltd. His specialty is in the area of industrial power system design and analysis, with emphasis on harmonics, the application and protection of large motors, and the design of substations and grounding. He has written several computer programs in the areas of motor starting, fault analysis, load flow analysis, and harmonic analysis. He has taught industrial power system design, advanced fault analysis, and protective relaying courses at the undergraduate and graduate levels at the University of Alberta.

Mr. Grainger is a senior member of the IEEE and a Registered Professional Engineer in the province of Alberta.

Roy C. Spencer (M'90) received the engineering degree from the Council of Engineering Institutions, London, UK in 1976, and the M.Eng. degree in electrical engineering from the University of Alberta in 1990.

He has worked in the mining, telecommunications, petrochemical, pipeline, and consulting industries and is an Engineering Specialist with Interprovincial Pipe Line Inc. His specialty is in the area of project management and industrial power and control systems, with emphasis on high-voltage systems and variable frequency drives.

Mr. Spencer is a Chartered Engineer in the U.K. and is a Registered Professional Engineer in the Province of Alberta.